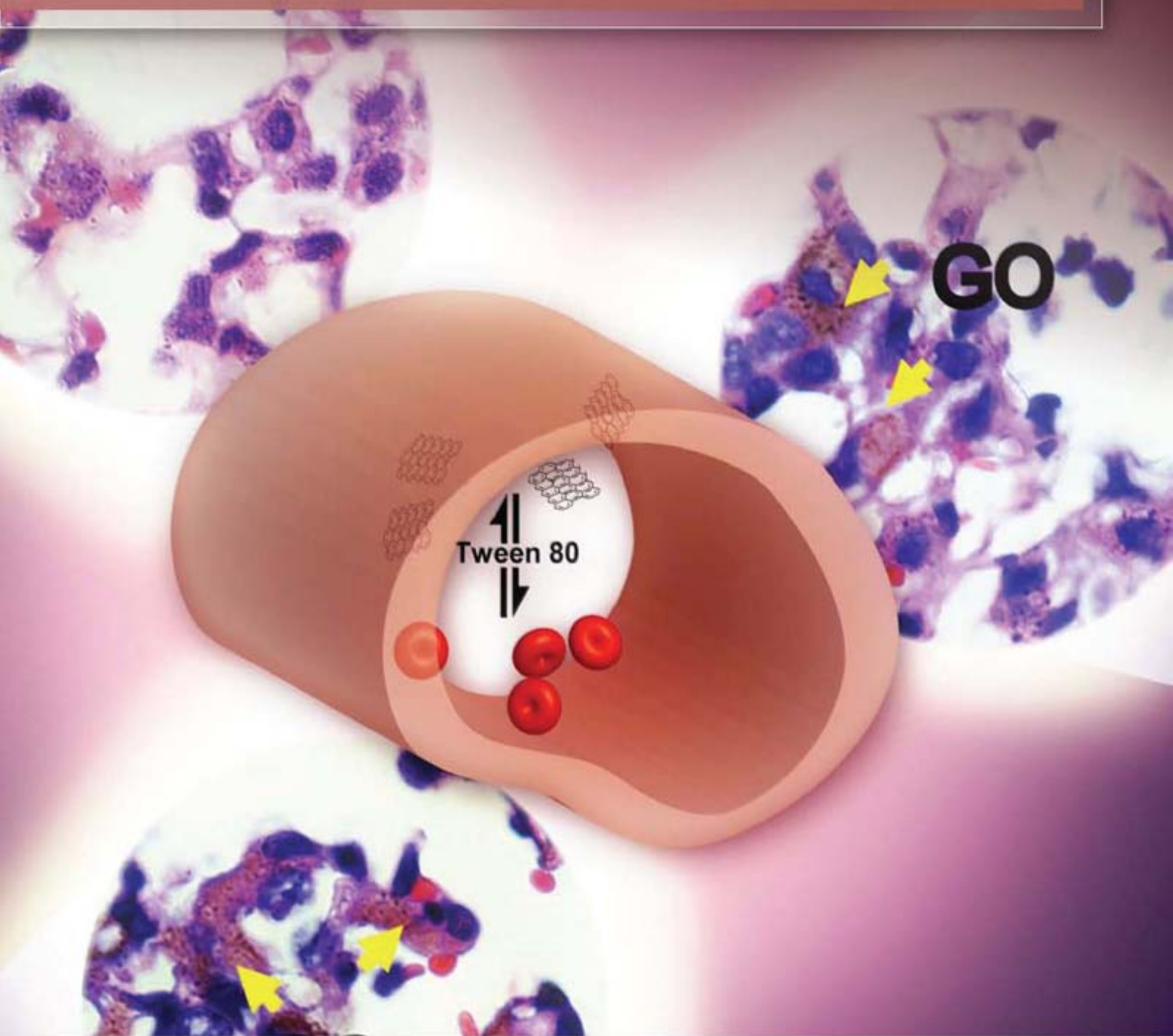


# JES

JOURNAL OF  
ENVIRONMENTAL  
SCIENCES

ISSN 1001-0742  
CN 11-2529/X

May 1, 2013 Volume 25 Number 5  
[www.jesc.ac.cn](http://www.jesc.ac.cn)



Sponsored by  
Research Center for Eco-Environmental Sciences  
Chinese Academy of Sciences

## CONTENTS

### Environmental biology

Continuous live cell imaging of cellulose attachment by microbes under anaerobic and thermophilic conditions  
using confocal microscopy

Zhi-Wu Wang, Seung-Hwan Lee, James G. Elkins, Yongchao Li, Scott Hamilton-Brehm, Jennifer L. Morrell-Falvey ..... 849

Response of anaerobes to methyl fluoride, 2-bromoethanesulfonate and hydrogen during acetate degradation

Liping Hao, Fan Lü, Lei Li, Liming Shao, Pinjing He ..... 857

Effect of airflow on biodrying of gardening wastes in reactors

F. J. Colomer-Mendoza, L. Herrera-Prats, F. Robles-Martínez, A. Gallardo-Izquierdo, A. B. Piña-Guzmán ..... 865

### Environmental health and toxicology

The *ex vivo* and *in vivo* biological performances of graphene oxide and the impact of surfactant on graphene  
oxide's biocompatibility (Cover story)

Guangbo Qu, Xiaoyan Wang, Qian Liu, Rui Liu, Nuoya Yin, Juan Ma, Liquan Chen, Jiuyang He, Sijin Liu, Guibin Jiang ..... 873

Determination of the mechanism of photoinduced toxicity of selected metal oxide nanoparticles (ZnO, CuO, Co<sub>3</sub>O<sub>4</sub> and  
TiO<sub>2</sub>) to *E. coli* bacteria

Thabitha P. Dasari<sup>1</sup>, Kavitha Pathakoti<sup>2</sup>, Huey-Min Hwang ..... 882

Joint effects of heavy metal binary mixtures on seed germination, root and shoot growth, bacterial bioluminescence,  
and gene mutation

In Chul Kong ..... 889

### Atmospheric environment

An online monitoring system for atmospheric nitrous acid (HONO) based on stripping coil and ion chromatography

Peng Cheng, Yafang Cheng, Keding Lu, Hang Su, Qiang Yang, Yikan Zou, Yanran Zhao,

Huabing Dong, Limin Zeng, Yuanhang Zhang ..... 895

Formaldehyde concentration and its influencing factors in residential homes after decoration at Hangzhou, China

Min Guo, Xiaoqiang Pei, Feifei Mo, Jianlei Liu, Xueyou Shen ..... 908

### Aquatic environment

Flocculating characteristic of activated sludge flocs: Interaction between Al<sup>3+</sup> and extracellular polymeric substances

Xiaodong Ruan, Lin Li, Junxin Liu ..... 916

Speciation of organic phosphorus in a sediment profile of Lake Taihu II. Molecular species and their depth attenuation

Shiming Ding, Di Xu, Xiuling Bai, Shuchun Yao, Chengxin Fan, Chaosheng Zhang ..... 925

Adsorption of heavy metal ions from aqueous solution by carboxylated cellulose nanocrystals

Xiaolin Yu, Shengrui Tong, Maofa Ge, Lingyan Wu, Junchao Zuo, Changyan Cao, Weiguo Song ..... 933

Synthesis of mesoporous Cu/Mg/Fe layered double hydroxide and its adsorption performance for arsenate in aqueous solutions

Yanwei Guo, Zhiliang Zhu, Yanling Qiu, Jianfu Zhao ..... 944

Advanced regeneration and fixed-bed study of ammonium and potassium removal from anaerobic digested wastewater  
by natural zeolite

Xuejun Guo, Larry Zeng, Xin Jin ..... 954

Eutrophication development and its key regulating factors in a water-supply reservoir in North China	
Liping Wang, Lusan Liu, Binghui Zheng .....	962
Laboratory-scale column study for remediation of TCE-contaminated aquifers using three-section controlled-release potassium permanganate barriers	
Baoling Yuan, Fei Li, Yanmei Chen, Ming-Lai Fu .....	971
Influence of Chironomid Larvae on oxygen and nitrogen fluxes across the sediment-water interface (Lake Taihu, China)	
Jingge Shang, Lu Zhang, Chengjun Shi, Chengxin Fan .....	978
Comparison of different phosphate species adsorption by ferric and alum water treatment residuals	
Sijia Gao, Changhui Wang, Yuansheng Pei .....	986
Removal efficiency of fluoride by novel Mg-Cr-Cl layered double hydroxide by batch process from water	
Sandip Mandal, Swagatika Tripathy, Tapswani Padhi, Manoj Kumar Sahu, Raj Kishore Patel .....	993
Determining reference conditions for TN, TP, SD and Chl- <i>a</i> in eastern plain ecoregion lakes, China	
Shouliang Huo, Beidou Xi, Jing Su, Fengyu Zan, Qi Chen, Danfeng Ji, Chunzi Ma .....	1001
Nitrate in shallow groundwater in typical agricultural and forest ecosystems in China, 2004–2010	
Xinyu Zhang, Zhiwei Xu, Xiaomin Sun, Wenyi Dong, Deborah Ballantine .....	1007
Influential factors of formation kinetics of flocs produced by water treatment coagulants	
Chunde Wu, Lin Wang, Bing Hu, Jian Ye .....	1015
<b>Environmental catalysis and materials</b>	
Characterization and performance of Pt/SBA-15 for low-temperature SCR of NO by C <sub>3</sub> H <sub>6</sub>	
Xinyong Liu, Zhi Jiang, Mingxia Chen, Jianwei Shi, Wenfeng Shangguan, Yasutake Teraoka .....	1023
Photo-catalytic decolourisation of toxic dye with N-doped titania: A case study with Acid Blue 25	
Dhruba Chakraborty, Susmita Sen Gupta .....	1034
Pb(II) removal from water using Fe-coated bamboo charcoal with the assistance of microwaves	
Zengsheng Zhang, Xuejiang Wang, Yin Wang, Siqing Xia, Ling Chen, Yalei Zhang, Jianfu Zhao .....	1044
Serial parameter: CN 11-2629/X*1989*m*205*en*P*24*2013-5	



## Flocculating characteristic of activated sludge flocs: Interaction between $\text{Al}^{3+}$ and extracellular polymeric substances

Xiaodong Ruan, Lin Li, Junxin Liu\*

Research Center for Eco-Environmental Science, Chinese Academy of Sciences, Beijing 100085, China. E-mail: [ruxido@163.com](mailto:ruxido@163.com)

Received 11 October 2012; revised 27 February 2013; accepted 04 March 2013

### Abstract

Aluminum flocculant can enhance the flocculating performance of activated sludge. However, the binding mechanism of aluminum ion ( $\text{Al}^{3+}$ ) and extracellular polymeric substances (EPS) in activated sludge is unclear due to the complexity of EPS. In this work, three-dimensional excitation emission matrix fluorescence spectroscopy (3DEEM), fluorescence quenching titration and Fourier transform infrared spectroscopy (FT-IR) were used to explore the binding behavior and mechanism between  $\text{Al}^{3+}$  and EPS. The results showed that two fluorescence peaks of tyrosine- and tryptophan-like substances were identified in the loosely bound-extracellular polymeric substances (LB-EPS), and three peaks of tyrosine-, tryptophan- and humic-like substances were identified in the tightly bound-extracellular polymeric substances (TB-EPS). It was found that these fluorescence peaks could be quenched with  $\text{Al}^{3+}$  at the dosage of 3.0 mg/L, which demonstrated that strong interactions took place between the EPS and  $\text{Al}^{3+}$ . The conditional stability constants for  $\text{Al}^{3+}$  and EPS were determined by the Stern-Volmer equation. As to the binding mechanism, the  $-\text{OH}$ ,  $\text{N}-\text{H}$ ,  $\text{C}=\text{O}$ ,  $\text{C}-\text{N}$  groups and the sulfur- and phosphorus-containing groups showed complexation action, although the groups in the LB-EPS and TB-EPS showed different behavior. The TB-EPS have stronger binding ability to  $\text{Al}^{3+}$  than the LB-EPS, and TB-EPS play an important role in the interaction with  $\text{Al}^{3+}$ .

**Key words:** extracellular polymeric substances; activated sludge; aluminum ion; three-dimensional excitation emission matrix; fluorescence quenching; Fourier transform infrared spectroscopy

**DOI:** 10.1016/S1001-0742(12)60210-1

### Introduction

The activated sludge process is the main wastewater treatment process in the world. The structural composition of activated sludge flocs can be mainly categorized as microorganisms, extracellular (More et al., 2012). Extracellular polymeric substances (EPS) are a kind of polymeric material produced by microorganisms under certain environmental conditions. It is known that EPS are responsible for protecting microorganisms in sludge flocs from external environment changes and also provide the material for binding cells and other particulate materials together and stabilizing the sludge floc structure (Liu et al., 2007; Martinez et al., 2004). EPS in activated sludge has a double layer structure with rheological properties, divided into loosely-bound EPS (LB-EPS) and tightly-bound EPS (TB-EPS) (Shao et al., 2010). The LB-EPS are located on the outer part of sludge floc at low density with rheological properties, and the TB-EPS are closely attached to the cell

wall at high density.

Aluminum flocculants (poly-aluminum and aluminum chloride) are typically used to improve the settling and dewatering properties of activated sludge (Agridiotis et al., 2007; Park et al., 2010). In addition, aluminum salts can help to aid in removal of phosphorus and suspended solids (Auvray et al., 2006; Omoike and VanLoon, 1999). Therefore, aluminum ion ( $\text{Al}^{3+}$ ) is widely distributed in sludge flocs. Now a growing number of researchers have noticed that the EPS is responsible for the movement and transformation of metal ions in wastewater treatment systems. Some researchers found that EPS has a huge surface area and a negative charge on its surface, and can undergo complexation reactions with a variety of metal ions, such as Cd, Ni, and Zn (Guibaud et al., 2009; Zheng et al., 2008). It has been reported that the content of  $\text{Al}^{3+}$  in the TB-EPS fraction has a higher ratio compared to other fractions in activated sludge. The concentration of  $\text{Al}^{3+}$  in TB-EPS and LB-EPS is 4.99 and 0.03 mg/L respectively, and the quantity of  $\text{Al}^{3+}$  in the TB-EPS accounts for 97.5% of the total content of  $\text{Al}^{3+}$  in activated sludge (Yu et

\* Corresponding author. E-mail: [jxliu@rcees.ac.cn](mailto:jxliu@rcees.ac.cn)

al., 2009). However, till now the binding properties and the binding mechanism of  $\text{Al}^{3+}$  and EPS have remained unclear because of the complexity of EPS. Data on the binding constants of EPS with  $\text{Al}^{3+}$  are still not available.

Three-dimensional excitation emission matrix fluorescence spectroscopy (3DEEM), also known as excitation-emission matrix, provides a versatile, rapid, and sensitive method for studying fluorescent organic compounds, and provides the spectra of fluorescence intensity changes with excitation (Ex) and emission (Em) wavelength changes simultaneously (Yamashita and Tanoue, 2003). In addition, 3DEEM can identify and characterize a multi-component complex system of overlapping objects in fluorescence spectra with high selectivity, high information content, and without destroying the sample structure (Shao et al., 2010). At present, 3DEEM has been successfully applied for analyzing some water components and polymers with metal cations such as the interaction properties of algal biofilm extracellular polymers with  $\text{Hg}^{2+}$  (Zhang et al., 2010), the binding behavior of humic substances with  $\text{Hg}^{2+}$  (Chai et al., 2012), and the interaction of acetamiprid with extracellular polymeric substances from activated sludge (Song et al., 2010).

The objective of this study is to investigate the binding behavior and mechanism of  $\text{Al}^{3+}$  with LB-EPS/ TB-EPS. The binding capacities and stability constants of EPS-Al were also determined by fluorescence quenching titration and analysis using the modified Stern-Volmer equation. Finally, the mechanism for the interaction of EPS-Al was also characterized by Fourier transform infrared spectroscopy (FT-IR). The extended knowledge presented here has significance for understanding the nature of EPS from activated sludge and the function of aluminum salts in activated sludge treatment systems.

## 1 Materials and methods

### 1.1 Extraction of EPS and determination of EPS components

Activated sludge was obtained from the Qinghe Municipal Sewage Treatment Plant in Beijing, China. The LB-EPS and TB-EPS were extracted following previous research (Yu et al., 2009), with minor modification. Briefly, the original sludge was washed with Milli-Q water and then centrifuged at  $4000 \times g$  for 5 min. It was resuspended in warm 0.05% NaCl (W/V) solution at  $50^\circ\text{C}$  and then sheared by a vortex mixer (Maxi Mix II, Thermolyne) for 1 min. The sample was centrifuged at  $4000 \times g$  for 10 min and the resulting supernatant liquid was regarded as the LB-EPS. The residue was re-suspended to the original volume using 0.05% NaCl (W/V), heated to  $60^\circ\text{C}$  in a water bath for 30 min, and then centrifuged at  $4000 \times g$  for 15 min. The extracted fraction in the supernatant was regarded as the TB-EPS. Both the LB-EPS and TB-EPS extraction solutions were analyzed by a total organic

carbon (TOC) analyzer (TOC-5000A, Shimadzu, Japan) to quantify TOC concentration. The protein content was determined by the modified Lowry method with bovine serum albumin as the standard (Frolund et al., 1995). Carbohydrate content was measured using the Anthrone method with glucose as the standard (Trevelyan et al., 1952).

### 1.2 Fluorescence measurements

The 3DEEM spectra of the LB-EPS and TB-EPS solution were carried out with a fluorescence spectrophotometer (F-4500, Hitachi, Japan) using a 150 W xenon arc lamp as the excitation source. The 3DEEM spectra were collected at 5 nm increments over an excitation wavelength range  $\lambda_{\text{Ex}} = 200\text{--}450$  nm, with an emission wavelength range  $\lambda_{\text{Em}} = 250\text{--}600$  nm every 2 nm. The excitation and emission slits were set to 5 and 10 nm of band-pass, respectively. The scan speed was 2400 nm/min and the response time was automatic. The extracted LB-EPS and TB-EPS were diluted and the samples placed in a 1 cm quartz cell before fluorescence scanning. The 3DEEM data was processed using the software FL Solutions Ver 2.0 (Hitachi, Japan). All experiments were conducted in duplicate and the mean values were used.

### 1.3 Influence of pH on fluorescence properties

Ten milliliters each of the LB-EPS and TB-EPS solutions in 50 milliliter glass vials were used to measure fluorescence in the presence of 3.0 mg/L of  $\text{Al}^{3+}$  in the samples at various pH. The pH of the EPS solution was adjusted in the range of 2.0 to 13.0 by adding high concentrations of KOH and  $\text{HNO}_3$  solution with an automatic syringe to avoid the effects of concentration dilution.

### 1.4 Fluorescence quenching titration

Three milliliters of EPS solution (7.5 mg/L) in a 22 mL glass vial was titrated with incremental additions of 0.1 mol/L  $\text{AlCl}_3$  solution at room temperature. By adding  $\text{AlCl}_3$  solution, the  $\text{Al}^{3+}$  concentration in glass vials was varied from 3 to 150  $\mu\text{mol/L}$ . The pH of the sample solution was adjusted to  $\text{pH } 4.00 \pm 0.05$  by the addition of 0.1 mol/L HCl or 0.1 mol/L NaOH, with the added reagent not exceeding 50  $\mu\text{L}$ . These samples were placed in darkness and shaken for 24 hr; after that, the 3DEEM and synchronous fluorescence emission spectra were measured using a fluorescence spectrophotometer (F-4500, Hitachi, Japan). The synchronous fluorescence emission spectra were obtained with fixed excitation wavelength 230, 280, and 350 nm, and fluorescence emission in the range of 250–450 nm and 5 nm slit widths.

### 1.5 Infrared sample preparation

FT-IR spectroscopy determined the infrared absorption spectrum of the samples, which provided a variety of structure information about the vibration and reactivity of



functional groups of the molecules in EPS. After the complexation reaction between  $\text{Al}^{3+}$  and LB-EPS/TB-EPS, the samples were lyophilized, then ground into powder in the light of a 60 W infrared lamp. The samples were mixed with potassium bromide (KBr) at a mass ratio of 1:150 and compressed into a thin disc using a hydraulic press at 8 MPa pressure. The spectral analysis of the composites was carried out using an FT-IR spectrometer (TENSOR 27, Bruker) in the range of 400–4000 nm. Infrared spectral data analysis was processed using Origin 7.5 software.

## 2 Results and discussion

### 2.1 Fluorescence characterization of LB-EPS and TB-EPS

The 3DEEM spectra of the LB-EPS and TB-EPS in the absence of  $\text{Al}^{3+}$  are shown in **Fig. 1**. Two distinct fluorescence peaks (A and B) were identified in the 3DEEM spectra of the LB-EPS sample (**Fig. 1a1**), while three distinct fluorescence peaks (C, D, and E) were identified in the TB-EPS sample (**Fig. 1b1**). The excitation and emission wavelengths showed that peak A and peak D were in the same location, and peak B and peak E were basically in

the same site. However, TB-EPS had a fluorescence peak C, which LB-EPS did not have. According to previous studies, peak A (Ex/Em = 230/300 nm) and peak D (Ex/Em = 230/300) were identified as tyrosine-like substances; peak B (Ex/Em = 280/350) and peak E (Ex/Em = 280/350) were identified as tryptophan-like substances; and peak C (Ex/Em = 350/440) was identified as visible region humus-like substances (Fellman et al., 2009; Flemming and Wingender, 2001).

The fluorescence intensities of peak A and peak D were significantly higher than the other fluorescence peaks, which may be attributable to the higher concentrations of protein contained in the EPS. The contents of protein and polysaccharides in TB-EPS (247.56 mg/g EPS, and 132.67 mg/g EPS) were much higher than those in LB-EPS (94.82 mg/g EPS and 73.86 mg/g EPS). Besides, the proteins/polysaccharides ratio for TB-EPS was 1.87, which was higher than the ratio for LB-EPS (1.30). Due to some proteins and amino acids, such as tryptophan and phenylalanine, which have strong fluorescent effects, peak A and peak D were the main fluorophores in the EPS sample (Wu and Tanoue, 2001). The fluorescence intensity of peak C was much less than the other four peaks, which signified that the amount of humus-like substances was

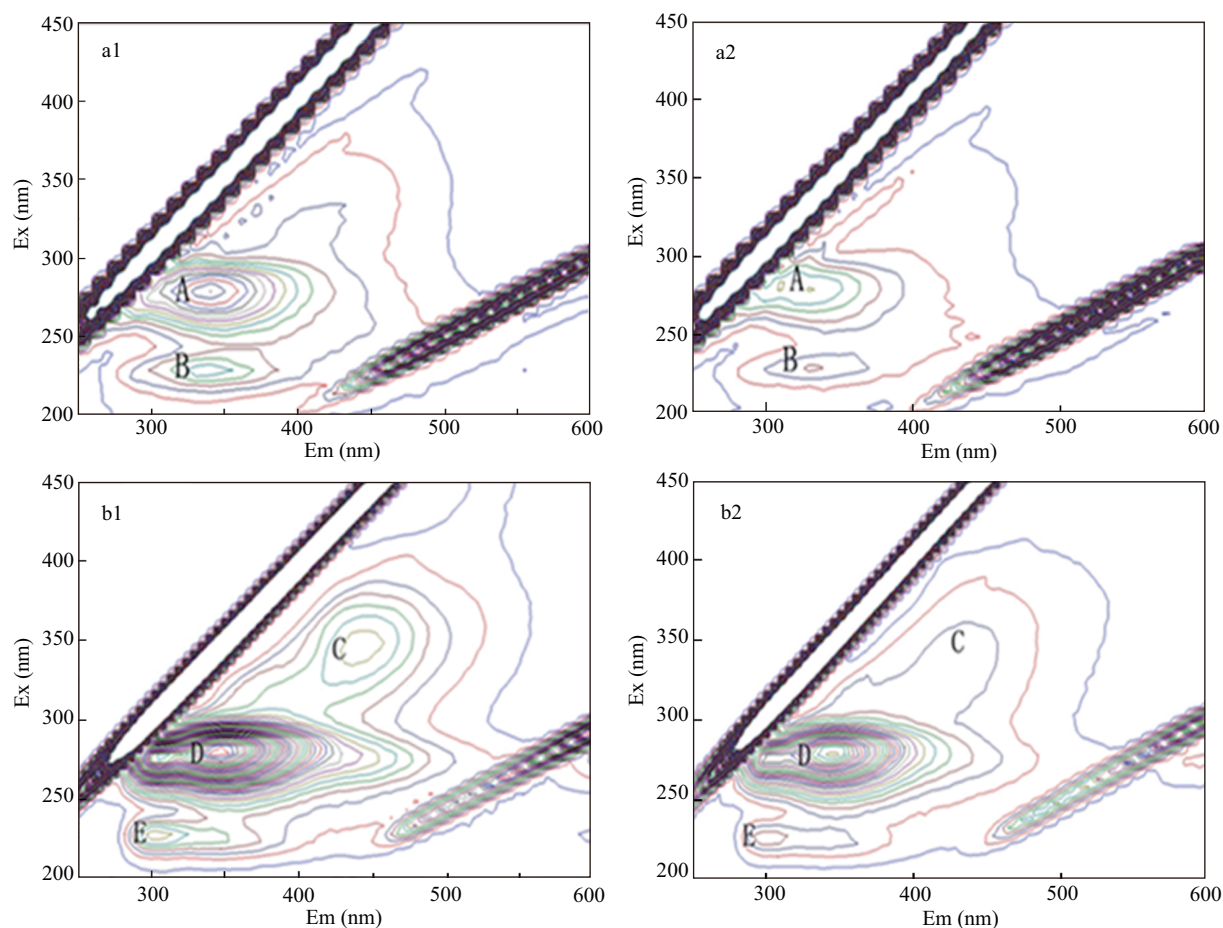


**Fig. 1** Typical 3DEEM spectra of LB-EPS (a) and TB-EPS (b) in the absence (a1 and b1) and presence (a2 and b2) of  $\text{Al}^{3+}$  ( $1.2 \times 10^{-5}$  mol/L) at pH 4.0. Peaks A and D: tyrosine-like substances; peaks B and E: tryptophan-like substances; peak C: humus-like substances.

much less than the other protein class substances.

## 2.2 EPS fluorescence quenching by $\text{Al}^{3+}$

As shown in 3DEEM of the LB-EPS and TB-EPS, the excitation wavelengths of the five fluorescence peaks were 230 nm (peak A and peak D), 280 nm (peak B and peak E) and 350 nm (peak C), so the synchronous fluorescence emission spectra were set with fixed excitation wavelengths of 230, 280, and 350 nm, thus to investigate the binding behavior of  $\text{Al}^{3+}$  and LB-EPS/ TB-EPS. The significant fluorescence quenching of the five fluorescence peaks for EPS in the presence of  $\text{Al}^{3+}$  are shown in **Fig. 1a2** and **1b2**. The fluorescence intensities decreased for both LB-EPS and TB-EPS on addition of  $\text{Al}^{3+}$ , indicating that  $\text{Al}^{3+}$  could interact with EPS and quench their intrinsic fluorescence. The quenching process always results from complexation between the fluorophore and quencher (Chai et al., 2012).

Due to the speciation of  $\text{Al}^{3+}$ , deprotonation of the functional groups of the polymer and the secondary structure of the protein are all influenced by the pH value. Thus, it was important to probe the fluorescence quenching titration of  $\text{Al}^{3+}$  under various pH conditions. As seen in **Fig. 2**, the fluorescence intensities of the five peaks in the 3DEEM spectra were strongly influenced by pH changes when the concentration of  $\text{Al}^{3+}$  was  $1.2 \times 10^{-5}$  mol/L. The insert figure shows peak D for the fluorescence intensity, which was much stronger than the other four peaks. When pH increased from 2.0 to 4.0, the fluorescence intensities of peaks A, B, D, and E showed a downward trend, but the trend was not obvious; and when pH increased from 4.0 to 6.0, the fluorescence intensities of these four peaks decreased rapidly, indicating that  $\text{Al}^{3+}$  had strong interaction with protein-like substances. However, peak C showed a different trend compared to the other peaks. The fluorescence intensity of peak C increased with pH increas-

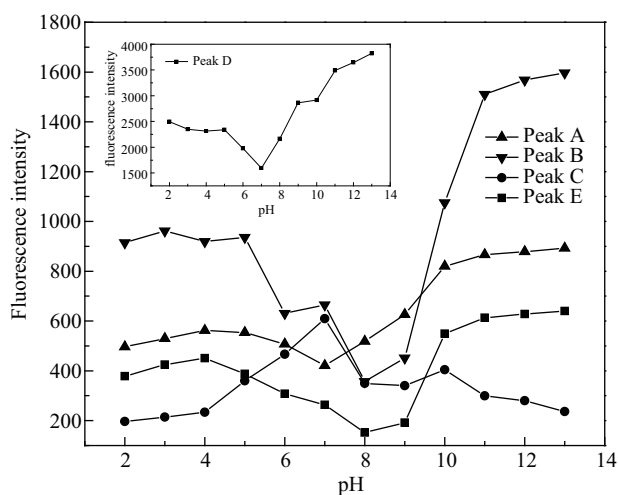


**Fig. 2** Effect of solution pH on fluorescence intensity of  $\text{Al}^{3+}$  and LB-EPS/TB-EPS ( $\text{Al}^{3+}$ :  $1.2 \times 10^{-5}$  mol/L). Values represent mean values of two independent measurements.

ing from 5.0 to 7.0, indicating that humic-like substances had a relatively weak interaction with  $\text{Al}^{3+}$  when pH ranged from 5.0 to 7.0. When pH further increased from 7.0 to 13.0, the fluorescence intensity of peak C displayed a downward trend, but the fluorescence intensities of peak A, B, D, and E increased gradually.

In aqueous solution, pH is one of the main parameters that influence the form of  $\text{Al}^{3+}$ . In general, when pH is between 2.0 to 4.0, Al exists mainly as free  $\text{Al}^{3+}$  ions; when pH is between 4.0 to 7.0, Al exists in the form of cations such as  $\text{Al}^{3+}$ ,  $\text{Al}(\text{OH})^{2+}$ , and  $\text{Al}_8(\text{OH})_{20}^{4+}$ ; when pH is between 7.0 to 9.0, Al exists mainly in the form of anions, such as  $\text{Al}(\text{OH})_4^-$ ; and when pH exceeds 9.0,  $\text{Al}^{3+}$  hydrolyses into  $\text{AlO}_2^-$ , which has weak complexation with fluorophores (Shen, 2002). This could explain why the protein-like substances in the LB-EPS and TB-EPS had strong complexation with  $\text{Al}^{3+}$  in the pH range 4.0 to 7.0. The relatively strong fluorescence quenching effects observed in the pH range 4.0 to 7.0 may be caused by the competition among  $\text{Al}^{3+}$ ,  $\text{Al}(\text{OH})^{2+}$ , and  $\text{Al}_8(\text{OH})_{20}^{4+}$  for complexation with the polymer functional groups. Because protein is the principal structural component of EPS, the isoelectric point of EPS is always in the acid pH range. As the zeta potential plot of the LB-EPS and TB-EPS solutions shows in **Fig. 3**, the isoelectric points were all at about pH 2.0. The zeta potential value decreased with increasing pH and gradually became stable at pH 6.0–13.0. With the pH moves away from the isoelectric point, the compact structure of EPS may become weak due to electrostatic repulsion and structural rearrangements, further leading to swelling and the release of chains, thus increasing the availability of binding sites to  $\text{Al}^{3+}$  (Wang et al., 2012). For peak A, B, D, and E, which belong to protein-like substances, the downward fluorescence intensity trend may be partly for the above-mentioned reason. However, in pH 8.0–13.0, the hydrolyzate of  $\text{AlO}_2^-$  from  $\text{Al}^{3+}$ , which has low affinity with fluorophores, was the main reason for

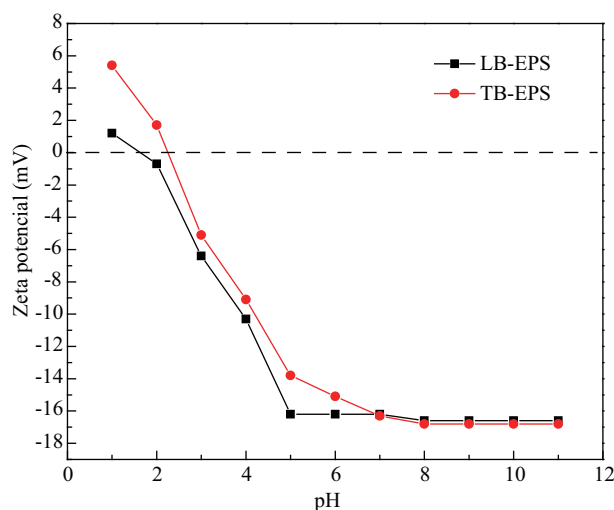


**Fig. 3** Zeta potential plot of LB-EPS and TB-EPS solutions versus pH. Values represent mean values of two independent measurements.

the low fluorescence quenching observed in **Fig. 2** and the upward fluorescence intensity trend. Additionally, the competition between hydroxyl and  $\text{AlO}^{2-}$  for binding sites may have also contributed to this phenomenon. Compared with peaks A, B, D, and E, which have comparatively lower fluorescence intensities in the range of pH 6.0–8.0, the fluorescence intensities of peak C showed the highest value in this pH range. The clearly distinct trend of peak C fluorescence intensity versus pH compared with the other four peaks may be caused by the competition between protons and  $\text{Al}^{3+}$  ions for the binding sites, and the coiled structure of the humus-like substances may also have prevented the access of  $\text{Al}^{3+}$ . Moreover, the hydrolyzate of  $\text{Al}^{3+}$  at acid or alkaline conditions may have weak fluorescence quenching effects on the different functional groups of humus-like substances. The same trend was also observed in previous research on the complexation between mercury and humic substances (Chai et al., 2012; Zhang et al., 2010).

### 2.3 Conditional stability constants for $\text{Al}^{3+}$ and EPS

$\text{Al}^{3+}$  exists mainly in the form of cations in the pH range of 2.0 to 4.0, and with the increase of pH, the form of  $\text{Al}^{3+}$  hydrolyzed to negatively charged anions (Shen, 2002). To quantify the quenching effect of different concentrations of  $\text{Al}^{3+}$  on the EPS, a series of synchronous fluorescence quenching titrations were conducted for the LB-EPS/TB-EPS with various concentrations of  $\text{Al}^{3+}$  at pH 4.0.

As shown in **Fig. 4**, all five fluorescence peaks were significantly quenched by  $\text{Al}^{3+}$  at pH 4.0, and the fluorescence of all peaks were remarkably quenched by 60  $\mu\text{mol/L}$  of  $\text{Al}^{3+}$ . The value of  $F/F_0$ , which was the ratio of fluorescence intensity of the peaks in the presence and absence of the quencher ( $\text{Al}^{3+}$ ), clearly showed substantial concave-down features in plots of  $F/F_0$  vs.  $\text{Al}^{3+}$  concentration.

Normally, the Stern-Volmer equation shows a linear profile (Zhao and Nelson, 2005). Interestingly, a distinct-

ly atypical concave-down response was observed in the Stern-Volmer equation of both the LB-EPS and TB-EPS. The concave-down response indicated the presence of two populations of fluorophores with unequal accessibility to the quencher (Zhao and Nelson, 2005), one of which could be accessible to the quencher, and another that could not. The appearance of a non-linear Stern-Volmer plot resulted from the fluorescence of the accessible fluorophore quenched by the addition of the quencher. Comparing the  $F/F_0$  value at  $\text{Al}^{3+}$  concentration 60  $\mu\text{mol/L}$  (**Fig. 4**), the fluorescence intensities of peaks A and B were about 40% quenched; however, over 50% of the fluorescence intensities were quenched for peak D and E, which indicated that the ratio of fluorophore populations accessible to the quencher was greater in the TB-EPS than that in the LB-EPS. According to the earlier analysis of the chemical composition of the LB-EPS and TB-EPS, it can be inferred that incomplete quenching of these five fluorescence peaks was partly because of their complex composition. Additionally, the proteins and humic substance in the EPS were a mixture in which binding sites for  $\text{Al}^{3+}$  were manifold.

To quantitatively describe the  $\text{Al}^{3+}$ -EPS complexing behavior, the binding sites that caused the fluorescence quenching were assumed to form 1:1 complexes between the  $\text{Al}^{3+}$  and EPS (Da Silva et al., 1998; Ryan and Ventry, 1990). The modified Stern-Volmer equation was used to estimate the complexing parameters by fitting the titration results (Bai et al., 2008; Pan et al., 2010). The Stern-Volmer equation is as follows:

$$F_0/\Delta F = F_0/(F_0 - F) = 1/(f_a K_{a[\text{Al}]}) + 1/f_a \quad (1)$$

$$f_a = F_{0a}/(F_{0a} + F_{0b}) \quad (2)$$

$$F_0 = F_{0a} + F_{0b} \quad (3)$$

where,  $f_a$  is the proportion of binding fluorophores in the total fluorophores, and  $K$  is the conditional stability constant.  $F_{0a}$  is the fluorescence of the fluorophore moieties

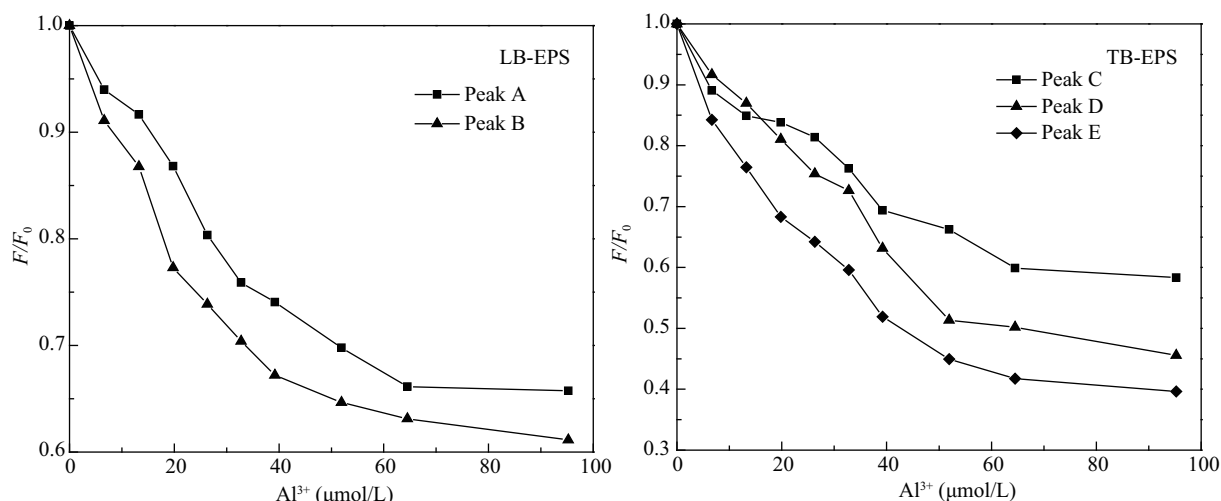


**Fig. 4**  $\text{Al}^{3+}$  quenching titration with different fluorescent peaks. The fluorescence of all five peaks were markedly quenched by 60  $\mu\text{mol/L}$  of  $\text{Al}^{3+}$ . Values represent mean values of two independent measurements.



that can complex with quencher and  $F_{0b}$  is the fluorescence of the inaccessible fluorophore moieties.

If the plot of  $F_0/(F_0-F)$  vs.  $1/[\text{Al}^{3+}]$  is a straight line,  $K$  and  $f_a$  values can be estimated from the slope ( $1/K_a$ ) and intercept ( $1/f_a$ ) (Esteves da Silva et al., 1998).

The modified Stern-Volmer plots of LB-EPS/TB-EPS titrations with  $\text{Al}^{3+}$  at pH 4.0 are shown in Fig. 5. All titration data of the protein-like peaks (A, B, D, and E) were well-fitted with the modified Stern-Volmer equation ( $R^2 = 0.9522-0.9858$ ). However, for the humic-like peak C,  $F_0/(F_0-F)$  vs.  $1/[\text{Al}^{3+}]$  showed a weak linear relationship ( $R^2 = 0.8811$ ,  $f_a = 0.3787$ ), indicating that the humic-like substances have different binding capacity for  $\text{Al}^{3+}$  compared to the other protein-like substances in EPS. The parameters,  $f_a$  and  $\log K_a$  of fluorophores of the five peaks were calculated.

The values of  $\log K_a$  for complexation of the five peaks in LB-EPS/TB-EPS with  $\text{Al}^{3+}$  are listed in Table 1. The maximum conditional stability constant for  $[\text{Al}^{3+}]/\text{EPS}$  was 4.7479 for peak C. The stability constants for the other peaks were between 4.1464–4.7479. In addition, the same types of fluorophores in LB-EPS and TB-EPS showed different stability constants for  $\text{Al}^{3+}$ . In the position of Ex/Em = 350 nm/440 nm, the stability constant of peak D for TB-EPS was greater than that of peak A for LB-EPS; and in the position of Ex/Em = 280 nm/350 nm, the stability constant of peak E (4.5859) for TB-EPS was much greater than that of peak B (4.3570) for LB-EPS, indicating that TB-EPS may have a stronger binding ability towards  $\text{Al}^{3+}$  than the LB-EPS. The  $f_a$  values of peaks A and B of the LB-EPS sample were close to each other; however, the values of  $f_a$  for peak D were significantly higher than for peak E and C in the TB-EPS sample. This indicated that the tyrosine-like substances had a higher proportion of binding fluorophores in the total fluorophores than the tryptophan-like and humus-like substances. Figure 1b1 shows that the fluorescence intensity of peak D was the strongest among

**Table 1** Complexation parameters of the peaks in 3DEEM spectra

Peaks	Ex/Em (nm/nm)	$\log K_a$	$f_a$	$R^2$
A	230/300	4.1464	0.6646	0.9522
B	280/350	4.3570	0.6623	0.9765
C	350/440	4.7479	0.3787	0.8811
D	230/300	4.1610	0.9120	0.9807
E	280/350	4.5859	0.7508	0.9858

the five peaks. These results demonstrated that the protein in the TB-EPS had good complexing capacity toward  $\text{Al}^{3+}$ , and the  $\text{Al}^{3+}$  in the wastewater treatment system may mostly exist in the EPS mass in complexed form. For peak C of the TB-EPS, the value of  $\log K_a$  was higher than that of the other peaks, suggesting higher complexation ability of humus-like substances than the protein-like substances, though the amount of humus was much lower than protein.

#### 2.4 Binding mechanism EPS- $\text{Al}^{3+}$

The previous studies showed that the protein and humic-like substances in EPS had strong interaction with  $\text{Al}^{3+}$ . However, the complexation reaction between  $\text{Al}^{3+}$  and LB-EPS/TB-EPS is influenced by pH, for the hydrolysis of  $\text{Al}^{3+}$  in water solution and the structure of the protein in EPS are both influenced by the pH value (Shen, 2002; Wang et al., 2012). Al exists mainly as free  $\text{Al}^{3+}$  ions only when pH is between 2.0 to 4.0, so to further understand the binding sites acted between  $\text{Al}^{3+}$  and the EPS, the FT-IR experiment was conducted to compare the LB-EPS/TB-EPS with or without  $\text{Al}^{3+}$  in the same condition of pH 4.0. As shown in Fig. 6, several absorption peaks that represent main functional groups could be observed. The peak around  $3400\text{ cm}^{-1}$  corresponded to O–H stretching, and the peak at  $2930\text{ cm}^{-1}$  was attributable to C–H stretching (Beech and Sunner, 2004). The peak at  $1636\text{ cm}^{-1}$  was assigned to the C=O stretching vibration in proteins Amide I, while the band near  $1394\text{ cm}^{-1}$  was

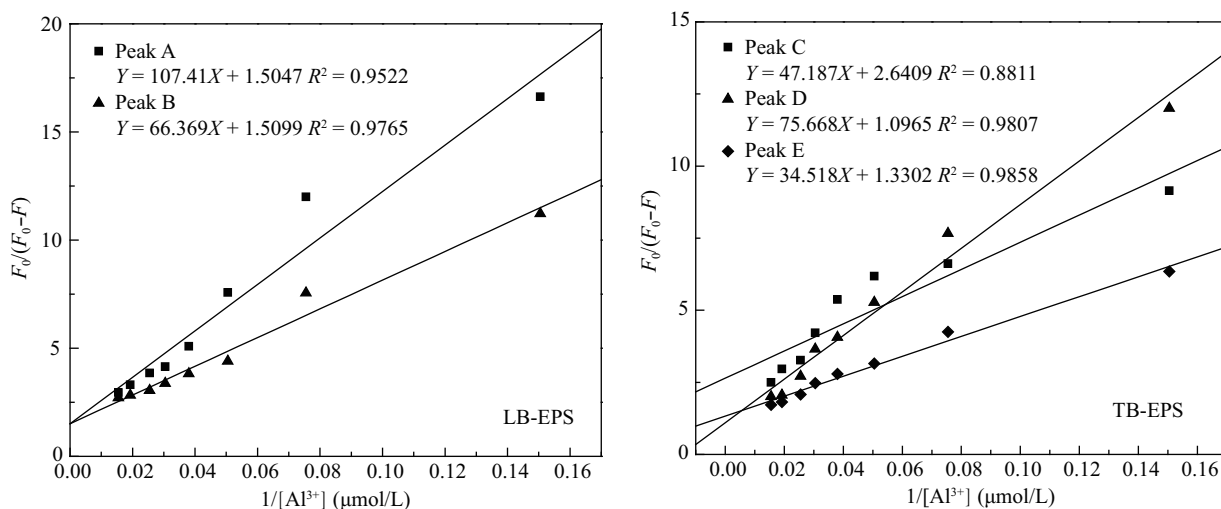


**Fig. 5** Modified Stern-Volmer plots of LB-EPS/TB-EPS titrations with  $\text{Al}^{3+}$  at pH 4.0. All titration data of the peaks A, B, D, and E were well-fitted with the modified Stern-Volmer equation. Peak C showed a weak linear relationship ( $R^2 = 0.8811$ ).

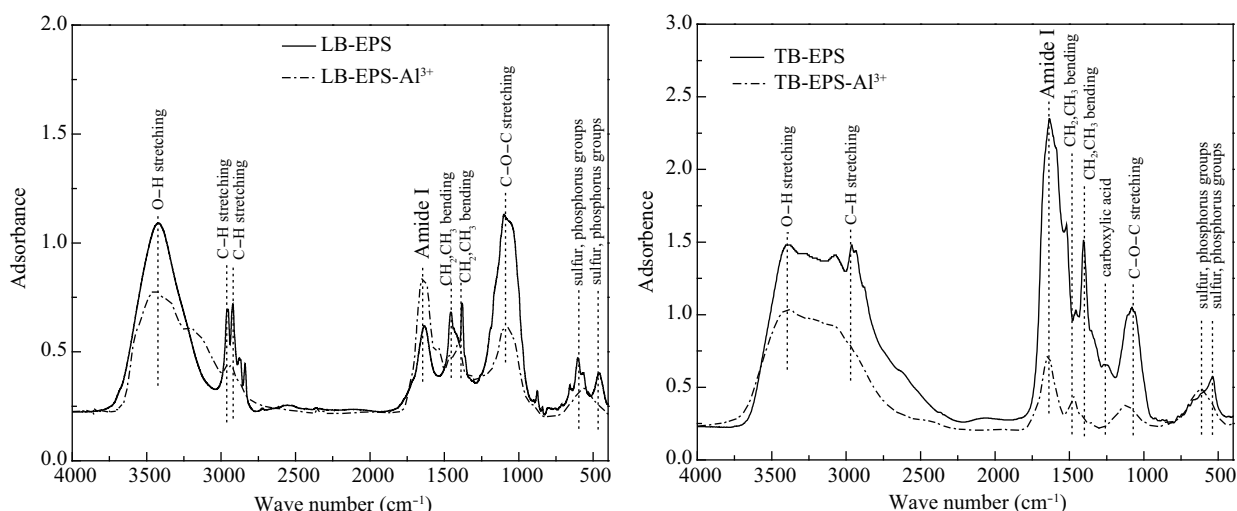


**Fig. 6** FT-IR spectra of LB-EPS and TB-EPS with or without  $\text{Al}^{3+}$ . The  $-\text{OH}$ ,  $\text{N}-\text{H}$ ,  $\text{C}=\text{O}$ ,  $\text{C}-\text{N}$  groups and the sulfur- and phosphorus-containing groups showed complexation action with  $\text{Al}^{3+}$ .

attributed to  $\text{CH}_2/\text{CH}_3$  symmetric stretching (Wang et al., 2012). The peak located at  $1150\text{--}1030\text{ cm}^{-1}$  originated from  $\text{C}-\text{O}-\text{C}$  stretching in polysaccharides (Merroun and Selenska-Pobell, 2008), and the peaks located at  $< 1000\text{ cm}^{-1}$  were attributed to  $\text{S}-\text{O}$  stretching or  $\text{P}-\text{O}$  stretching, known as the fingerprint area (Quiroz et al., 2006).

Within the FT-IR spectra in **Fig. 6**, some bands drifted or disappeared, summarized as follows: (1) In both LB-EPS and TB-EPS sample, the absorption intensity of  $-\text{OH}$  at  $3700\text{--}3000\text{ cm}^{-1}$  decreased and drifted. (2) In both LB-EPS and TB-EPS sample, the  $\text{C}-\text{H}$  stretching vibration at  $2963\text{--}2926\text{ cm}^{-1}$  assigned to aliphatic carbon chains decreased and the  $\text{CH}_2$  and  $\text{CH}_3$  stretching vibration at  $1455\text{ cm}^{-1}$  decreased remarkably. (3) In the TB-EPS sample, the  $\text{C}=\text{O}$  stretching vibration at  $1636\text{ cm}^{-1}$  assigned to Amide I proteins decreased; the stretching vibration at  $1394\text{ cm}^{-1}$  assigned to  $\text{CH}_2/\text{CH}_3$  experienced a red shift and moved to  $1471\text{ cm}^{-1}$ ; and the  $\text{C}=\text{O}$  vibration at  $1250\text{ cm}^{-1}$  assigned to carboxylic acid disappeared. (4) In the TB-EPS sample, the  $\text{O}-\text{H}$  stretching vibration at  $1074\text{ cm}^{-1}$  assigned to alcohols or carboxyl experienced a blue shift to  $1011\text{ cm}^{-1}$ . (5) In LB-EPS sample, the  $\text{C}-\text{O}-\text{C}$  stretching vibration at  $1074\text{ cm}^{-1}$  assigned to polysaccharides decreased. (6) In the fingerprint area at  $< 1000\text{ cm}^{-1}$ , the spectra of LB-EPS and TB-EPS varied significantly after complexation. For LB-EPS, the bands at  $596$  and  $457\text{ cm}^{-1}$  disappeared, while a new band at  $567\text{ cm}^{-1}$  appeared. For TB-EPS, the band at  $531\text{ cm}^{-1}$  moved to  $634\text{ cm}^{-1}$ .

The FT-IR analysis showed that the main groups located on proteins in the EPS, including  $\text{C}=\text{O}$ ,  $\text{C}-\text{N}$ ,  $-\text{OH}$ , and amide groups, reacted with  $\text{Al}^{3+}$ , which may be via electrostatic interaction. Furthermore, the  $\text{C}-\text{O}-\text{C}$  group on polysaccharides,  $-\text{OH}$  assigned to alcohols or carboxyl,  $\text{C}=\text{O}$  belonging to carboxyl or phenolic alcohols, and the sulfur- and phosphorus-containing groups were also involved in the complexation reaction. These results indicated that, although the protein-like and humic-

like substances had strong binding capacity for  $\text{Al}^{3+}$ , the polysaccharides, DNA, phosphate, and sulfate groups may also provide binding sites for  $\text{Al}^{3+}$ .

The above experimental results indicate that, during the activated sludge flocculation process with aluminum salts,  $\text{Al}^{3+}$  functions by interaction with proteins, humic-like substances and polysaccharides in EPS, among which the proteins and humic-like substances have relatively strong complexing capability with  $\text{Al}^{3+}$ .  $\text{Al}^{3+}$  could bind with the functional groups, i.e.  $-\text{OH}$ ,  $\text{N}-\text{H}$ ,  $\text{C}=\text{O}$  and  $\text{C}-\text{N}$  in EPS, thus to (1) neutralize the negative charge of the EPS and decrease the repulsion forces between the polymeric substances, (2) bridge connecting multiple molecules. Therefore, the floc structure can be more compact and could further improve the settling properties and the dewatering properties of sludge flocs (Agridiotis et al., 2007; Park et al., 2010). A conclusion that TB-EPS is the main complexation agent could be gained due to the greater complexation ability and greater amount of TB-EPS than LB-EPS, which could explain the phenomenon of the higher ratio of  $\text{Al}^{3+}$  in the TB-EPS fraction compared to other fractions in activated sludge mentioned in the literature (Yu et al., 2009).

3DEEM and synchronous fluorescence technology are only applicable for fluorescent components (e.g., proteins and humic acids), but not for other components that do not emit fluorescence, such as polysaccharides, phosphate and sulfate. Polysaccharides are important binding sites for metals (Guibaud et al., 2009; Zhang et al., 2006). Besides, uronic acids, DNA, and phosphate may also be involved in binding with cations (Quiroz et al., 2006; Beech and Sunner, 2004). Thus, to obtain a comprehensive understanding of the mechanisms involved in the complexation of EPS with  $\text{Al}^{3+}$ , other methods such as extended X-ray absorption fine structure analysis, nuclear energy resonance, and time of Flight mass spectrometry need to be complementarily used in the future.

### 3 Conclusion

Fluorescence peaks of tyrosine- and tryptophan-like substances were identified from the LB-EPS and TB-EPS samples, respectively. A fluorescence peak of humic-like substances was also identified in the TB-EPS sample. The fluorescence of the five peaks was significantly quenched by  $\text{Al}^{3+}$ , indicating the presence of complexes formed between EPS and  $\text{Al}^{3+}$ . The values of conditional stability constants ( $\log K_a = 4.1464\text{--}4.7479$ ) derived from the modified Stern-Volmer equation were appropriate to those for protein-like and humic-like peaks. The tyrosine-like substances had a higher proportion of binding fluorophores than the tryptophan-like and humus-like substances. Aluminum ions showed complexation action with  $-\text{OH}$ ,  $\text{N}-\text{H}$ ,  $\text{C}=\text{O}$ ,  $\text{C}-\text{N}$  groups and the sulfur- and phosphorus-containing groups, but a significant difference was observed in the number and types of the groups for complexation between the LB-EPS and TB-EPS. The TB-EPS had stronger binding ability to  $\text{Al}^{3+}$  than the LB-EPS, and played an important role in the interaction with  $\text{Al}^{3+}$ .

### Acknowledgments

This work was funded by the National Natural Science Foundation of China (No. 51138009, 50921064). The technical assistance of Mr. Wang Yinjie from the Institute of Process Engineering, Chinese Academy of Science, and Ms. Li Ang'zhen from the Research Center for Eco-Environmental Science, Chinese Academy of Sciences is highly appreciated.

### References

- Agridiotis V, Forster C F, Carliell M C, 2007. Addition of Al and Fe salts during treatment of paper mill effluents to improve activated sludge settlement characteristics. *Biore-source Technology*, 98(15): 2926–2934.
- Alvarado Quiroz N G A, Hung C C, Santschi P H, 2006. Binding of thorium(IV) to carboxylate, phosphate and sulfate functional groups from marine exopolymeric substances (EPS). *Marine Chemistry*, 100(3–4): 337–353.
- Auvray F, Van Hullebusch E D, Deluchat V, Baudu M, 2006. Laboratory investigation of the phosphorus removal (SRP and TP) from eutrophic lake water treated with aluminium. *Water Research*, 40(14): 2713–2719.
- Bai Y C, Wu F C, Wan G J, Liu C Q, Fu P Q, Li W, 2008. Ultraviolet absorbance titration for the determination of conditional stability constants of  $\text{Hg}(\text{II})$  and dissolved organic matter. *Chinese Journal of Geochemistry*, 27(1): 46–52.
- Beech I B, Sunner J, 2004. Biocorrosion: towards understanding interactions between biofilms and metals. *Current Opinion in Biotechnology*, 15(3): 181–186.
- Chai X L, Liu G X, Zhao X, Hao Y X, Zhao Y C, 2012. Complexion between mercury and humic substances from different landfill stabilization processes and its implication for the environment. *Journal of Hazardous Materials*, 209–210(0): 59–66.
- Da Silva J C G E, Machado A A S C, Oliveira C J S, Pinto M S S D S, 1998. Fluorescence quenching of anthropogenic fulvic acids by  $\text{Cu}(\text{II})$ ,  $\text{Fe}(\text{III})$  and  $\text{UO}_2^{(2+)}$ . *Talanta*, 45(6): 1155–1165.
- Fellman J B, Miller M P, Cory R M, D'Amore D V, White D, 2009. Characterizing dissolved organic matter using PARAFAC modeling of fluorescence spectroscopy: a comparison of two models. *Environmental Science and Technology*, 43(16): 6228–6234.
- Flemming M C, Wingender J, 2001. Relevance of microbial extracellular polymeric substances (EPS), Part I: structural and ecological aspects. *Water Science and Technology*, 43(6): 1–8.
- Frolund B, Griebe T, Nielsen P H, 1995. Enzymatic activity in the activated-sludge floc matrix. *Applied Microbiology and Biotechnology*, 43(4): 755–761.
- Guibaud G, Van Hullebusch E, Bordas F, d'Abzac P Joussein E, 2009. Sorption of  $\text{Cd}(\text{II})$  and  $\text{Pb}(\text{II})$  by exopolymeric substances (EPS) extracted from activated sludges and pure bacterial strains: Modeling of the metal/ligand ratio effect and role of the mineral fraction. *Bioresource Technology*, 100(12): 2959–2968.
- Liu Y, Li J, Qiu X F, Burda C, 2007. Bactericidal activity of nitrogen-doped metal oxide nanocatalysts and the influence of bacterial extracellular polymeric substances (EPS). *Journal of Photochemistry and Photobiology A: Chemistry*, 190(1): 94–100.
- Martínez O F, Felipe Lema J, Méndez R, Cuervo-López F, Gómez J, 2004. Role of exopolymeric protein on the settleability of nitrifying sludges. *Bioresource Technology*, 94(1): 43–48.
- Merroun M L, Selenska-Pobell S, 2008. Bacterial interactions with uranium: an environmental perspective. *Journal of Contaminant Hydrology*, 102(3–4): 285–95.
- More T T, Yan S, John R P, Tyagi R D, Surampalli R Y, 2012. Biochemical diversity of the bacterial strains and their biopolymer producing capabilities in wastewater sludge. *Bioresource Technology*, 121: 304–311.
- Omoike A I, VanLoon G W, 1999. Removal of phosphorus and organic matter removal by alum during wastewater treatment. *Water Research*, 33(17): 3617–3627.
- Pan X L, Liu J, Zhang D Y, 2010. Binding of phenanthrene to extracellular polymeric substances (EPS) from aerobic activated sludge: A fluorescence study. *Colloids and Surfaces B: Biointerfaces*, 80(1): 103–106.
- Park C, Fang Y, Murthy S N, Novak J T, 2010. Effects of floc aluminum on activated sludge characteristics and removal of 17- $\alpha$ -ethinylestradiol in wastewater systems. *Water Research*, 44(5): 1335–1340.
- Ryan D K, Ventry L S, 1990. Exchange of comments on fluorescence quenching measurements of copper–fulvic acid binding. *Analytical Chemistry*, 62(14): 1523–1526.
- Shao L M, Wang G Z, Xu H C, Yu G H, He P J, 2010. Effects of ultrasonic pretreatment on sludge dewaterability and extracellular polymeric substances distribution in mesophilic anaerobic digestion. *Journal of Environmental Sciences*, 22(3): 474–480.
- Shen Z, Zhao Z G, Wang G T, 2002. *Colloids and Surface Chemistry*. Chemical Industry Press, Beijing.
- Song W J, Mu G J, Zhang D Y, Pan X L, 2010. Interaction of

- acetamidiprid with extracellular polymeric substances (EPS) from activated sludge: A fluorescence study. *African Journal of Biotechnology*, 9(45): 7667–7673.
- Trevelyan W E, Forrest R S, Harrison J S, 1952. Determination of yeast carbohydrates with the anthrone reagent. *Nature*, 170(4328): 626–627.
- Wang L L, Wang L F, Ren X M, Ye X D, Li W W, Yuan S J et al., 2012. pH dependence of structure and surface properties of microbial EPS. *Environmental Science and Technology*, 46(2): 737–744.
- Wu F C, Tanoue E, 2001. Isolation and partial characterization of dissolved copper–complexing ligands in stream waters. *Environmental Science and Technology*, 35(18): 3646–3652.
- Yamashita Y, Tanoue E, 2003. Chemical characterization of protein–like fluorophores in DOM in relation to aromatic amino acids. *Marine Chemistry*, 82(3–4): 255–271.
- Yu G H, He P J, Shao L M, 2009. Characteristics of extracellular polymeric substances (EPS) fractions from excess sludges and their effects on biofloculability. *Bioresource Technology*, 100(13): 3193–3198.
- Zhang D Y, Pan X L, Mostofa K M G, Chen X, Mu G, Wu F et al., 2010. Complexation between Hg(II) and biofilm extracellular polymeric substances: An application of fluorescence spectroscopy. *Journal of Hazardous Materials*, 175(1–3): 359–365.
- Zhang D L, Wang J L, Pan X L, 2006. Cadmium sorption by EPSs produced by anaerobic sludge under sulfate–reducing conditions. *Journal of Hazardous Materials*, 138(3): 589–593.
- Zhao J, Nelson D J. 2005. Fluorescence study of the interaction of Suwannee River fulvic acid with metal ions and  $\text{Al}^{3+}$ –metal ion competition. *Journal of Inorganic Biochemistry* 99(2): 383–396.
- Zheng L, Ding A Z, Wang J S, Tian Y, 2008. Adsorption of Cd(II), Zn(II) by extracellular polymeric substances extracted from waste activated sludge. *Water Science and Technology*, 58(1): 195–200.

# JOURNAL OF ENVIRONMENTAL SCIENCES

环境科学学报(英文版)  
(<http://www.jesc.ac.cn>)

## Aims and scope

*Journal of Environmental Sciences* is an international academic journal supervised by Research Center for Eco-Environmental Sciences, Chinese Academy of Sciences. The journal publishes original, peer-reviewed innovative research and valuable findings in environmental sciences. The types of articles published are research article, critical review, rapid communications, and special issues.

The scope of the journal embraces the treatment processes for natural groundwater, municipal, agricultural and industrial water and wastewaters; physical and chemical methods for limitation of pollutants emission into the atmospheric environment; chemical and biological and phytoremediation of contaminated soil; fate and transport of pollutants in environments; toxicological effects of terrorist chemical release on the natural environment and human health; development of environmental catalysts and materials.

## For subscription to electronic edition

Elsevier is responsible for subscription of the journal. Please subscribe to the journal via <http://www.elsevier.com/locate/jes>.

## For subscription to print edition

China: Please contact the customer service, Science Press, 16 Donghuangchenggen North Street, Beijing 100717, China. Tel: +86-10-64017032; E-mail: [journal@mail.sciencep.com](mailto:journal@mail.sciencep.com), or the local post office throughout China (domestic postcode: 2-580).

Outside China: Please order the journal from the Elsevier Customer Service Department at the Regional Sales Office nearest you.

## Submission declaration

Submission of an article implies that the work described has not been published previously (except in the form of an abstract or as part of a published lecture or academic thesis), that it is not under consideration for publication elsewhere. The submission should be approved by all authors and tacitly or explicitly by the responsible authorities where the work was carried out. If the manuscript accepted, it will not be published elsewhere in the same form, in English or in any other language, including electronically without the written consent of the copyright-holder.

## Submission declaration

Submission of the work described has not been published previously (except in the form of an abstract or as part of a published lecture or academic thesis), that it is not under consideration for publication elsewhere. The publication should be approved by all authors and tacitly or explicitly by the responsible authorities where the work was carried out. If the manuscript accepted, it will not be published elsewhere in the same form, in English or in any other language, including electronically without the written consent of the copyright-holder.

## Editorial

Authors should submit manuscript online at <http://www.jesc.ac.cn>. In case of queries, please contact editorial office, Tel: +86-10-62920553, E-mail: [jesc@263.net](mailto:jesc@263.net), [jesc@rcees.ac.cn](mailto:jesc@rcees.ac.cn). Instruction to authors is available at <http://www.jesc.ac.cn>.

## Journal of Environmental Sciences (Established in 1989)

Vol. 25 No. 5 2013

<b>Supervised by</b>	Chinese Academy of Sciences	<b>Published by</b>	Science Press, Beijing, China
<b>Sponsored by</b>	Research Center for Eco-Environmental Sciences, Chinese Academy of Sciences		Elsevier Limited, The Netherlands
<b>Edited by</b>	Editorial Office of Journal of Environmental Sciences P. O. Box 2871, Beijing 100085, China Tel: 86-10-62920553; <a href="http://www.jesc.ac.cn">http://www.jesc.ac.cn</a> E-mail: <a href="mailto:jesc@263.net">jesc@263.net</a> , <a href="mailto:jesc@rcees.ac.cn">jesc@rcees.ac.cn</a>	<b>Distributed by</b>	
		Domestic	Science Press, 16 Donghuangchenggen North Street, Beijing 100717, China Local Post Offices through China
		Foreign	Elsevier Limited <a href="http://www.elsevier.com/locate/jes">http://www.elsevier.com/locate/jes</a>
<b>Editor-in-chief</b>	Hongxiao Tang	<b>Printed by</b>	Beijing Beilin Printing House, 100083, China
<b>CN 11-2629/X</b>	<b>Domestic postcode: 2-580</b>	<b>Domestic price per issue</b>	<b>RMB ¥ 110.00</b>

ISSN 1001-0742



9 771001 074130